submitted to PRL

Mechanisms of Photo Double Ionization of Helium by 530 eV Photons

A. Knapp[1], A. Kheifets[2], I. Bray[3], Th. Weber[1], A. L. Landers[4], S. Schössler[1], T. Jahnke[1], J. Nickles[1], S. Kammer[1], O. Jagutzki[1], L. Ph. Schmidt[1], T. Osipov[5], J. Rösch[6,1], M. H. Prior[6], H. Schmidt-Böcking[1], C. L. Cocke[5] and R. Dörner[1*]

[1] *Institut für Kernphysik, Universität Frankfurt, August-Euler-Str. 6, D-60486 Frankfurt, Germany*
[2] *Research School of Physical Sciences and Engineering, Australian National University Canberra ACT 0200, Australia*
[3] *Centre for Atomic, Molecular and Surface Physics, Murdoch University, Perth, 6150 Australia*
[4] *Dept. of Physics, Western Michigan Univ., Kalamazoo, MI 49008*
[5] *Dept. of Physics, Kansas State Univ., Cardwell Hall, Manhattan KS 66506*
[6] *Lawrence Berkeley National Lab., Berkeley CA 94720*

(Dated: November 30, 2001)

We have measured fully differential cross sections for photo double ionization (PDI) of helium 450 eV above the threshold. We have found an extremely asymmetric energy sharing between the photoelectrons and an angular asymmetry parameter $\beta \simeq 2$ and $\beta \simeq 0$ for the fast and slow electrons, respectively. The electron angular distributions show a dominance of the shake-off mechanism for 2 eV electrons and clear evidence of an inelastic electron-electron scattering at 30 eV. The data are in excellent agreement with CCC calculations.

How does a single photon couple to two electrons in an atom? This question has been extensively discussed in the literature. Most of this discussion has been focused on the photo double ionization (PDI) of the helium atom which is the simplest two-electron-single-photon process (see McGuire et al. [1] and Briggs and Schmidt [2] for reviews). It is generally believed that at high photon energies the shake-off mechanism makes the largest contribution to PDI. The shake-off is a relaxation of the correlated initial state onto the new He^+ eigenstates after a sudden removal of one atomic electron. In contrast, close to the threshold, mainly one electron absorbs the photon and knocks out the second electron in an (e,2e) like collision (the process which is called in the literature the two-step-one, or TS1). This dominance of the TS1 mechanism is supported by the experimental observation of Samson [3] that the ratio of the total double to total single ionization cross-sections is proportional to the cross section for electron impact ionization of the He^+ ion from the threshold up to an excess energy of $\simeq$ 200 eV. In the high photon energy limit, however, the ratio converges to a constant $R = 1.67$ %, a limit expected for the shake-off [4, 5]. The whole discussion on the PDI mechanisms is based solely on theory [6–9] and on measured total cross sections [3].

Detailed experimental and theoretical studies of the angular and energy correlation between the two photoelectrons or, equivalently, the photoelectron and the recoiling ion are presently available in the form of the fully resolved triple differential cross section (TDCS) (see Briggs and Schmidt [2] for a recent review). However, these studies are limited to relatively low photon energies where the shake-off mechanism is believed to be not significant. Additionally, in this regime the angular distributions and the energy sharing are determined almost entirely by the long range Coulomb repulsion of the photoelectrons and the dipole selection rules, which completely mask the signatures of particular ionization mechanisms.

This Letter presents experimental data and theoretical calculations of PDI of helium at 530 eV photon energy where the shake-off yields a significant contribution. We show that characteristics of the shake-off and TS1 can be clearly seen in the TDCS. Electrons in the range of 2 eV are mainly produced by the shake-off while at 30 eV we find clear evidence of TS1. This confirms a theoretical prediction of Teng and Shakeshaft [9] who found that at high photon energies the ionization mechanism would leave clear signatures in the angular distribution. As we will show below, the virtue of such a study at high photon energies is that the two photoelectrons typically have very different energies and angular distributions, allowing experimental selection of the primary high energy electron which is coupled to the photon.

The experiment has been performed using the COLTRIMS technique (see [10] for a general review and [11, 12] for application to synchrotron radiation). The photon beam ($\hbar\omega = 529$ eV) from beamline 4 of the Advanced Light Source (ALS) at the Lawrence Berkeley National Laboratory is focussed into a supersonic helium gas jet. Electrons of energy below 60 eV are collected by a combination of electric and magnetic fields onto a large area position sensitive channel plate detector [13]. From the time of flight and the position of impact the momentum vector of the electron is deduced [14]. The electric field guides the ions with 4π collection solid angle for

*Electronic address: doerner@hsb.uni-frankfurt.de

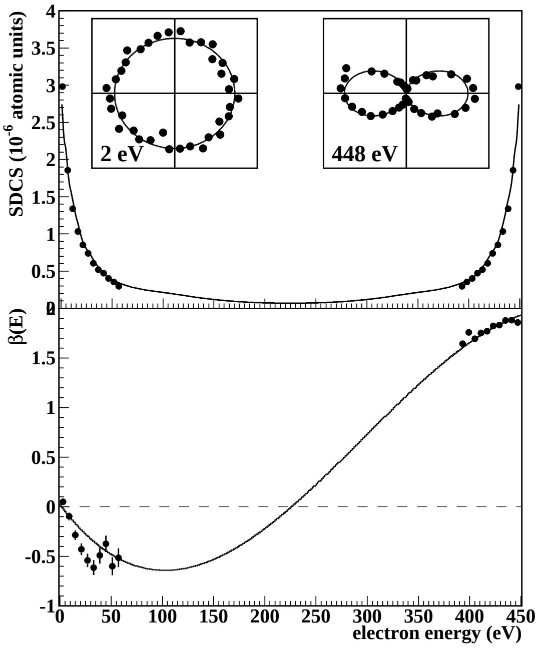

FIG. 1: DPI of He at $\hbar\omega = 529$ eV. a) SDCS $d\sigma/dE$. The line is the CCC calculation. The insets show the DDCS $d\sigma^2/(d\Omega dE)$ at $E = 2$ eV and 448 eV (the vertical axis is the light propagation), the line is obtained using Eq. (1), see text. The experimental data are normalized to the CCC calculation. b) The asymmetry parameter β versus the electron energy.

all momenta onto a second position sensitive detector. The ion charge state and momentum vector are again obtained from the time of flight and position of impact. The momentum vector of the fast electron is calculated from the measured slow electron and recoiling ion using momentum conservation.

The following observations present the arguments for a two-step picture in which one electron absorbs the photon energy and angular momentum and, subsequently, the second electron is either shaken-off or knocked out. We find an extremely asymmetric energy sharing and an angular asymmetry parameter $\beta \simeq 2$ for the fast electron. We then investigate the angular correlation between the photoelectrons and find that the very slow electrons (close to 2 eV) show a slight backward emission relative to the fast electron as expected from the shake-off. At the same time, the slow electrons at higher energy (20 eV and above) are mostly emitted at 90° to the fast electron indicating that a binary electron-electron collision is necessary to transfer this energy.

We corroborate our findings by performing a series of convergent close-coupling (CCC) calculations (see Kheifets and Bray [15] for details). In brief, the fast photoelectron of energy E_1 is described in the CCC model by a Coulomb wave whereas the slow photoelectron of energy E_2 is represented by a positive energy pseudostate of the He^+ ion. The shake-off mechanism is reproduced in the model by the dipole matrix element between a highly correlated ground state wave function and a product of the Coulomb wave E_1 and the pseudostate E_2. The TS1 mechanism is represented by the inelastic scattering of the fast electron on an eigen- or pseudostate of the ion. The amplitude of this process is calculated as a non-diagonal element of the scattering T-matrix. The diagonal part of the T-matrix describes the elastic electron scattering in which the quantum state of the slow electron does not change. The only effect of this elastic scattering is the distortion of the Coulomb wave representing the fast electron, and so is attributed to the shake-off mechanism [7].

We calculate a succession of cross-sections starting from the fully-resolved TDCS $d^3\sigma/(d\Omega_1 d\Omega_2\, dE_1)$. Integrating the TDCS over $d\Omega_2$ reduces it to the double differential cross-section (DDCS) which determines the energy and angular distribution of one photoelectron integrated over all angles of the second electron. Within the dipole approximation the DDCS is given by [16]

$$\frac{d^2\sigma}{d\Omega dE} = \frac{d\sigma}{dE}\frac{1}{4\pi}\Big[1+\beta(E)\Big(\frac{3}{2}\cos^2\vartheta - \frac{1}{2}\Big)\Big]. \quad (1)$$

Here $d\sigma/dE$ is the single differential cross-section (SDCS) which gives the energy sharing distribution between the photoelectrons, β is the angular asymmetry parameter and ϑ is the polar angle of the electron with respect to the polarization axis of light.

The top panel of Figure 1 shows the measured and calculated SDCS. It has a characteristic U-shape and peaks sharply at 0 eV and 450 eV. This trend is very well represented by the CCC calculation and has already been established in earlier calculations [9, 17, 18]. This run of the curve is in contrast to the SDCS close to the threshold which is almost flat.

The bottom panel of Figure 1 shows the measured and calculated β parameter. Note that at high incident energies, as is the present case, the CCC-calculated SDCS or β parameter cannot be readily determined with sufficient accuracy away from highly asymmetric energy sharing conditions. This is due to the sparseness of the pseudostate energy distribution. Therefore the solid lines in Figure 1 represent a polynomial interpolation through several explicitly calculated SDCS or β points. We verified the validity of the dipole approximation for the DDCS of Eq. (1) and did not find, within the statistical uncertainty, any significant forward-to-backward asymmetry in our data. Two examples of the experimental DDCS at $E = 2$ eV and 448 eV are shown in the insets together with the line obtained from Eq. (1), using CCC estimates of the SDCS and β. A very asymmetric energy sharing together with an angular asymmetry parameter $\beta \simeq 2$ indicate that the fast electron absorbs not only most of the photon energy but also the angular momentum. This directly suggests an interpretation of the DPI as a two-step process with the fast electron being the primary photoelectron. The slow electron is isotropic at

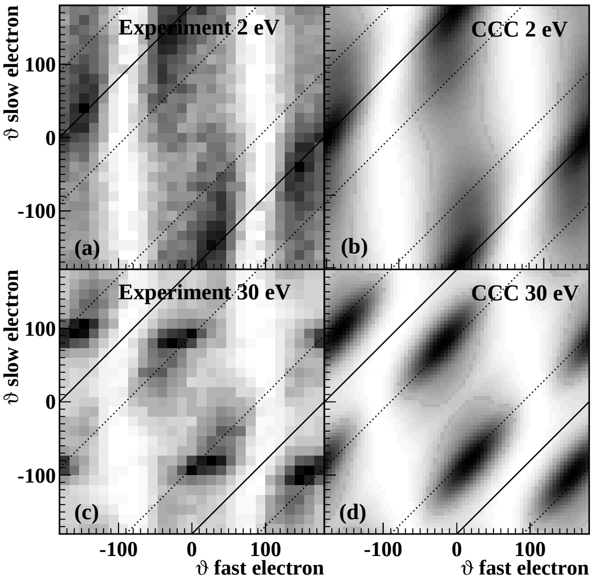

FIG. 2: Overview of the TDCS at 450 eV excess energy [(a) and (c) experiment, (b) and (d) CCC calculation] and coplanar emission for electron energies between 0 - 3 eV for the slow electrons (447 - 450 eV for the fast electron, respectively) (a,b) and 20 - 40 eV (410 - 430 eV) (c,d). The horizontal axis shows the angle ϑ_1 of the fast electron with respect to the polarization vector, the vertical axis displays the angle ϑ_2 of the slow electron. The full lines indicate the back-to-back emission $\vartheta_{12} = 180°$ (the shake-off), the dashed line defines emission of the two electrons of an angle $\vartheta_{12} = 90°$ as expected from the TS1 mechanism. Experimental data and theory are integrated over the same energy and angular range.

very low energy as expected for the shake-off while β becomes slightly negative for higher energies. As we will show below in more detail, this slightly preferred emission perpendicular to the polarization is a consequence of a binary encounter between the two electrons.

To learn more about the mechanism by which the second electron is emitted an overview of the TDCS of both electrons is given in Figure 2. The horizontal axis shows the polar angle ϑ_1 of the fast electron with respect to the polarization, the vertical axis displays the angle of the slow electron ϑ_2. Both electrons are chosen to be coplanar, i.e. the slow electron is within $\pm 35°$ in the plane defined by the fast electron and the polarization axis. The fast electron has almost no intensity at $\vartheta_1 = 90°$ reflecting a β parameter of close to 2, see Eq. (1). The two left panels show the experimental data whereas the corresponding right panels exhibit the TDCS from the CCC calculations. Good agreement between theory and experiment can be seen for all angles at both energy sharings.

In these two-dimensional plots the typical characteristics of the shake-off and TS1 mechanisms can be clearly identified. For the shake-off one would expect that the slow electron is emitted isotropically or slightly backwards to the fast primary electron. The locus of such events is indicated by the full line $\vartheta_{12} \equiv |\vartheta_1 - \vartheta_2| = 180°$. The TS1 is, in contrast, a binary encounter between two particles of equal mass, hence one expects it to peak at $\vartheta_{12} = 90°$. This is indicated by the dashed line also in Figure 2. At $E_2 = 2$ eV the maximum of the TDCS follows closely the $\vartheta_{12} = 180°$ lines supporting that such slow electrons are produced predominantly via shake-off. At $E_2 = 30$ eV the maxima are clearly along the lines with $\vartheta_{12} = 90°$, indicating a switch from the shake-off to a binary collision mechanism. A significant energy transfer from the primary to the secondary electron seems to require a binary collision and is not likely via the shake-off mechanism. It can be noted from the U-shaped SDCS (figure 1) that the contribution of the slow shake-off electrons to the total cross section is by far dominant over the electrons of 30 eV and higher. Thus the total DPI cross section is dominated by the shake-off process [7].

For a closer inspection and a detailed comparison with theory we have plotted a small subset of the data shown in Figure 2 as polar plots (figure 3). In all cases one of the electrons has been fixed to one direction within 10° of the linear polarisation, and the TDCS of the complementary electron is plotted. Thus data from figure 2 within the range $-10° < \vartheta_1 < 10°$ appear in Figure 2 (b) and (d), and in the range $-10° < \vartheta_2 < 10°$ are shown in Figure 2 (a) and (c). The TDCS for electrons $E_2 < 3$ eV (figure 3b) has a pear-like shape peaked at 180° to the fast electron. Contrary to all TDCS reported at lower photon energies so far, these slow electrons show a significant intensity for parallel emission into the same direction. This is possible because of the very asymmetric energy sharing of the two electrons. The solid line is a full CCC calculation which is in excellent agreement with the measurements. The dashed line is the CCC calculation representing the shake-off in which only the diagonal part of the T-matrix is retained. The corresponding TDCS of the fast electron ($E_1 > 447$ eV) shows a dipolar shape (Figure 3a) with the lobe for parallel emission into the same direction of the electrons being slightly suppressed.

The TDCS for electrons $E_2 \simeq 30$ eV (figure 3 c,d) are completely different from the low energy ones. We find emission of the electron into a narrow cone at 90° to the fast electron (figure 3 d). An angle of 90° between the electrons is expected from a binary collision between the electrons. Again the full CCC calculation is in very good agreement with the measurements. The shape of the shake-off only calculation is in complete disagreement with the data, the overall size however is comparable. The complete CCC calculation is a coherent sum of the shake-off and the TS1 contribution. Since the fast electron peaks parallel to the polarization, the 90° angle between the electrons also leads to a slightly negative β at these electron energies (see Figure 1b).

In conclusion, we have presented experimental and theoretical TDCS of the DPI of helium at the photon energy $\hbar\omega = 529$ eV (excess energy of 450 eV above the double ionization threshold). At such a high excess energy, with

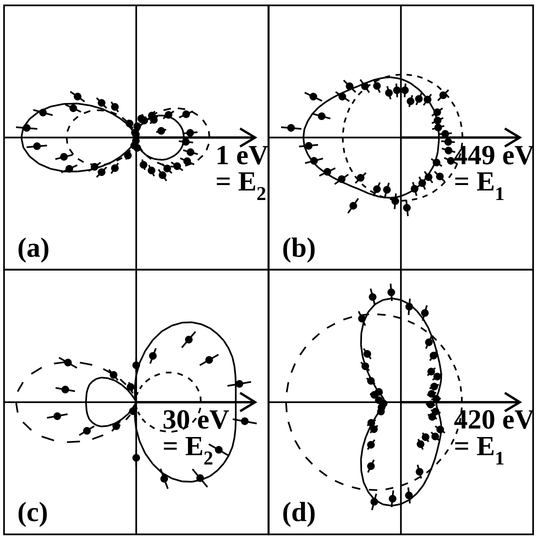

FIG. 3: TDCS of the He PDI at 529 eV photon energy. In all panels the electrons are coplanar within $\pm 25°$, the polarization axis (of linearly polarized light) is horizontal. The direction and the energy of one of the two electrons is fixed as indicated by the number and the arrow, i.e. the slow electron is fixed in (a) and (c) and the fast electron is fixed in (b) and (d). The polar plots show the angular distribution of the complementary electron. The upper panels (a) and (b) are for the case $E_2 \simeq$ 2 eV; the lower panels have $E_2 \simeq$ 30 eV. The solid line is a full CCC calculation, the dashed line is a shake-off only CCC calculation. The measurements are normalized to the full CCC calculation. Different linestyles are used to show calculation at the left and right quadrants of panel C; the shake-off calculation on the left side in (c) is multiplied by 0.4. The measurements and calculations are integrated over the same angular and energy ranges. a) $447 < E_1 < 450$ eV, $-10° < \vartheta_1 < 10°$, b) $0 < E_2 < 3$ eV, $-10° < \vartheta_2 < 10°$, c) $410 < E_1 < 430$ eV, $-10° < \vartheta_1 < 10°$, d) $20 < E_2 < 40$ eV, $-10° < \vartheta_2 < 10°$.

highly asymmetric kinematics we may think of the fast and slow electrons as being distinguishable. The angular distribution between the two electrons indicates that the very low energy secondary electrons are mostly emitted via the shake-off process while higher energy transfer requires a hard binary collision and leads to an angle of 90° between the electrons.

ACKNOWLEDGMENTS

This work was supported in part by BMBF, DFG, the Division of Chemical Sciences, Geosciences and Biosciences Division, Office of Basic Energy Sciences, Office of Science, U. S. Department of Energy and the Director, Office of Science, Office of Basic Energy Sciences. The computations were performed at the National Facility of the Australian Partnership for Advanced Computing. R. D. was supported by the Heisenberg Programm der DFG. A. K. and Th. W. thank Graduiertenförderung des Landes Hessen for financial support. Many thanks to E. Arenholz and T. Young and the staff of the ALS extraordinary support during our beam time. R. D. acknowledges many enlightening discussions with J. Berakdar, A. Becker and S. Keller.

REFERENCES

[1] J. McGuire, N. Berrah, R. Bartlett, J. Samson, J. Tanis, C. Cocke, and A. Schlachter, J. Phys. **B28**, 913 (1995).
[2] J. Briggs and V. Schmidt, J. Phys. **B33**, R1 (2000).
[3] J. Samson, Phys. Rev. Lett. **65**, 2861 (1990).
[4] J. Levin, D. Lindle, N. Keller, R. Miller, Y. Azuma, N. Mansour, H. Berry, and I. Sellin, Phys. Rev. Lett. **67**, 968 (1991).
[5] L. Spielberger, O. Jagutzki, R. Dörner, J. Ullrich, U. Meyer, V. Mergel, M. Unverzagt, M. Damrau, T. Vogt, I. Ali, et al., Phys. Rev. Lett. **74**, 4615 (1995).
[6] K. Hino, T. Ishihara, F. Shimizu, N. Toshima, and J.H. McGuire, Phys. Rev. **A48**, 1271 (1993).
[7] A. Kheifets, J. Phys. **B34**, L247 (2001).
[8] S. Keller, J. Phys. **B33**, L513 (2000).
[9] Z. Teng and R. Shakeshaft, Phys. Rev. **A49**, 3597 (1994).
[10] R. Dörner, V. Mergel, O. Jagutzki, L. Spielberger, J. Ullrich, R. Moshammer, and H. Schmidt-Böcking, Physics Reports **330**, 96 (2000).
[11] R. Dörner, J. Feagin, C. Cocke, H. Bräuning, O. Jagutzki, M. Jung, E. Kanter, H. Khemliche, S. Kravis, V. Mergel, et al., Phys. Rev. Lett. **77**, 1024 (1996), see also erratum in Phys. Rev. Lett. 78. 2031 (1997).
[12] R. Dörner, H. Bräuning, J. Feagin, V. Mergel, O. Jagutzki, L. Spielberger, T. Vogt, H. Khemliche, M. Prior, J. Ullrich, et al., Phys. Rev. **A57**, 1074 (1998).
[13] (see Roentdek.com for details of the detectors).
[14] R. Moshammer, J. Ullrich, M. Unverzagt, W. Schmitt, P. Jardin, R. Olson, R. Dörner, V. Mergel, and H. Schmidt-Böcking, Nucl. Instr. Meth. **B107**, 62 (1996).
[15] A. S. Kheifets and I. Bray, J. Phys. B **31**(10), L447 (1998).
[16] M. Y. Amusia, *Atomic photoeffect* (Plenum Press, New York, 1990).
[17] D. Proulx and R. Shakeshaft, Phys. Rev. **A48**, R875 (1993).
[18] M. Kornberg and J. Miraglia, Phys. Rev. **A48**, 3714 (1993).